J. Min. Metall. Sect. B-Metall. 59 (3) (2023) 375 - 382

Journal of Mining and Metallurgy, Section B: Metallurgy

PHASE TRANSFORMATION MECHANISM OF OXIDATION ROASTING OF LOW-GRADE POLYMETALLIC CHALCOPYRITE ORE IN THE PRESENCE OF CaO

H.-F. Ma, Y.-L. Liao *, M. Wu, X.-B. Jia, S.-Y. Yang

Faculty of Metallurgical and Energy Engineering, Kunming University of Science and Technology, Kunming, China

(Received 26 July 2023; Accepted 01 December 2023)

Abstract

Low-grade polymetallic chalcopyrite ore has a high lead and iron content and a low softening point, which is difficult to treat using conventional pyrometallurgical and hydrometallurgical processes. In order to investigate the suitable methodology for efficient utilization, it was pelletized with CaO for oxidation roasting in the present work. By controlling the Po_2 and Pso_2 in the gas phase, the metal sulfide in the ore was converted into easily soluble metal oxide, the thermal analysis of the roasting process was carried out and the acid leaching of the extracted calcine at atmospheric pressure was investigated. The results show that by pelletizing with CaO and then roasting at 800 °C for 1 h, chalcopyrite is converted into CuO, which can be easily dissolved, galena and pyrite are converted into PbO_2 and Fe_2O_3, respectively, and sulfur reacts with CaO and turns into $CaSO_4$, which can fix the sulfur in the calcine. The copper leaching rate of calcine can reach 98.60 wt.% under atmospheric pressure in the H_2SO_4-H_2O system. CaO can increase the softening point of raw materials, improve the roasting effect, promote the phase transformation of chalcopyrite in the oxidation process, and convert sulfur into $CaSO_4$ to fix sulfur, effectively avoiding SO_2 pollution to the environment.

Keywords: *Low grade chalcopyrite; Calcifying roasting; Oxidation roasting; Phase transition; Acid leaching*

1. Introduction

Chalcopyrite is the most abundant copper mineral, accounting for approximately 70% of the world's copper mineral resources [1]. However, with the continuous exploitation, high-grade copper minerals are increasingly depleted, resulting in a large number production of low-grade polymetallic complex chalcopyrite ore (LPCCO). LPCCO is characterized by low grade of copper, intergrowth and/or association of multiple metals, complex structure, and high content of lead and iron. Therefore, traditional pyrometallurgical processes for extracting copper are not suitable for the treatment of this kind of minerals [2]. Environmentally friendly hydrometallurgical processes have gradually become the main method for treating LPCCO [3-8], among which is microbial leaching [9-11] and pressure leaching [12-14] that have become research hotspots. Although the microbial leaching process of chalcopyrite is environmentally friendly and has good application prospects, it takes a long time and requires strict process control, making it difficult to achieve industrialization. The oxygen pressure acidic leaching method can destroy the special crystal structure of chalcopyrite and help to suppress the passivation layer appearing during the leaching process, it must be carried out under high temperature and pressure, with high energy consumption and low safety performance. To solve this problem, the method of thermal activation can be adopted to oxidize the insoluble $CuFeS_2$ into soluble CuS while treated by oxygen pressure acidic leaching. In addition, studies have shown that sulfide roasting pretreatment can significantly change the crystal structure of chalcopyrite, thereby improving its solubility in the acid leaching process [15, 16]. Although the sulfidation roasting followed by acid leaching process does not generate SO_2 and has the advantages of high copper leaching rate, this process requires completion in a sulfur atmosphere that is isolated from air, making it difficult to achieve in industrial applications with significant limitations. When using the traditional oxidation roasting process followed by acid leaching with dilute acid, the presence of low melting point components like lead in the raw material leads to softening and wrapping during the roasting process, resulting in incomplete oxidation of the internal metal sulfide phase, and a reduction in the leaching rate of copper while the roasted products are leached. Recent studies have shown that the addition of CaO can

Corresponding author: liaoyl@kust.edu.cn

https://doi.org/10.2298/JMMB230726032M

CC BY SA

improve the softening point of materials and promote the oxidation process of sulfides [17, 18]. This paper studies the phase transformation mechanism of oxidation roasting of LPCCO in the presence of CaO, providing a theoretical basis for effective utilizing LPCCO.

2. Experimental

2.1. Raw material

The raw material (LPCCO) used in this study was the secondary copper concentrate after flotation obtained from a mining company in Yunnan, China. The main chemical components contained in it are listed in Table 1. From Table 1, it can be seen that the metal elements account for about 56.42%, the element S accounts for about 30.00 wt.%, and other amorphous impurities account for 13.58 wt.%.

Table 1. *Mass composition of main elements in LPCCO*

Element	Cu	Pb	Fe	S	other
Content, wt.%	7.70	28.20	20.52	30.00	13.58

2.2. Experimental protocol

First, 100 g LPCCO, 50 g CaO (>99 wt.%), as well as 5 g deionized water were taken and mixed evenly to make a pellet with a specified particle diameter, then the obtained pellets were dried in an oven for drying to constant weight at temperature 105 ℃. Second, the dried pellets were placed in furnace to heat for 1 hour at temperature 800 ℃ in atmospheric environment, followed by crushing to obtain the calcine with a particle size less than 75 μm for leaching with diluted sulfuric acid while cooling to room temperature. Third, the calcine was leached and stirred at the speed of 500 r/min for 1.5 h at 85 ℃ in a 1 L three-necked bottle with the liquid-solid ratio of 5∶1 mL/g and mass concentration of sulfuric acid of 120 g/L, and the dosage of calcine used for each leaching was 100 g.

2.3. Characterization and analysis

The content of chemical elements in LPCCO and leaching residues were quantitatively determined using the Optima-5300DV ICP-AES spectrometer of Pekin Elmer Company (USA) while the samples were dissolved in acidity solution, and the copper content in the leachate obtained was determined by iodometry. The mineral phase of raw materials, calcined products and leaching residues were characterized by X-ray diffraction (XRD) using an X'Pert Pro MPD X-ray diffractometer. The operating parameters were tube voltage 40 kV, tube current 40 mA, scanning range 5° to 90°, and scanning speed 10°/min. JSM-6360 scanning electron microscope (SEM) equipped with X-ray energy dispersive spectroscopy (EDS) was used to analyze the morphology of raw materials, calcined products, and leaching residues.

3. Results and discussion

3.1. Thermodynamic analysis

Thermodynamic analysis of the oxidation roasting process of LPCCO was carried out, and the relevant chemical reactions. Their standard Gibbs free energy (Δ_rG^θ) and Gibbs free energy at temperatures between 473.15-1200 K ($\Delta_rG^\theta{}_{-T}$) during the roasting process are shown in Table 2. The thermodynamic data of all reactions listed in Table 2 were calculated using the thermodynamic database of HSC Chemistry 6.0 (HSC) software. It can be seen from Table 2 that under the same calcination conditions, the presence of calcium oxide (Equation 13) was more likely to occur than the absence of calcium oxide (Equation 4). The copper phase in the calcined product was mainly CuO rather than $CuFeO_2$. By comparing the Gibbs free energy of the oxidation reaction at 473.15-1200 K in the presence of CaO, it can be concluded that the oxidation order of related sulfides is: FeS_2>$CuFeS_2$>PbS. In addition, it can be seen from Table 2 that the free energy of the reaction Δ_rG^θ when adding CaO was more negative, indicating that the presence of CaO could promote the oxidation process of $CuFeS_2$, FeS_2, and PbS, and that CaO could also play a role in sulfur fixation.

To further illustrate the phase transition process of $CuFeS_2$, according to the content of $CuFeS_2$, FeS_2 and PbS in the raw material, an equilibrium component diagram of the oxidation process of LPCCO with a fixed content of $CuFeS_2$ 0.122 kmol, FeS_2 0.366 kmol, PbS 0.137 kmol, CaO 0.893 kmol was drawn using HSC software under air conditions. The equilibrium composition was determined by the Gibbs free energy minimization method under conditions of isothermal, isobaric, and fixed mass [19]. The equilibrium composition diagram of the oxidation reaction is shown in Figure 1.

As can be seen from Figure 1(a), in the range of 200-927 ℃ without CaO, copper mainly existed in the form of $CuSO_4$ when the reaction temperature was lower than 700 ℃. At this time, $FeCuS_2$ was oxidized according to the equation 2 in Table 2, resulting in the equilibrium component of $CuSO_4$ sharp decrease when the temperature was higher than 700 ℃. Instead, oxidation of $FeCuS_2$ should be carried out according to the equations (1) and (3) in Table 2. At this time, the copper phase began to transform from sulfate to oxide, which was consistent with the experimental results of Coruh [15]. From Figure 1(b), it can be seen that in the presence of CaO, within the temperature range of 200-929 ℃, $FeCuS_2$ mainly existed in the form of CuO, but as the temperature increased, a small amount of $CuO{\cdot}Fe_2O_3$ was generated, which was mainly oxidized

CC BY SA

according to equation (13) in Table 2. The above analysis shows that the phase transition of copper in LPPC was $CuFeS_2 \rightarrow CuSO_4 \rightarrow CuO{\cdot}Fe_2O_3 \rightarrow CuO$ within the temperature range of 200-929 °C, and that among of them CuO was the most stable phase [20].

In order to study the behavior of $CuFeS_2$, FeS_2, and PbS during oxidative roasting process at atmospheric environment in the presence of CaO, the dominant regions diagram of Cu-Fe-Ca-O-S, Pb-Ca-O-S, and Cu-Fe-Pb-O-S systems at 800 °C were plotted, then the dominant regions of Cu-Fe-Ca-O-S, Pb-Ca-O-S and Cu-Fe-Pb-O-S systems were obtained by superposition diagram [21, 22, 23], which were shown in Figure 2. As can be seen from Figure 2, in the presence of CaO, the stable phases of the Cu-Fe-Ca-O-S system were CuO, Fe_2O_3, and $CaSO_4$, while

Table 2. *Related chemical reactions and standard Gibbs free energy of mineral phase reconstruction process at 473.15-1200 K*

No.	Reaction equation	Δ_rG^θ/kJ	$\Delta_rG^\theta{}_{-T}$/ kJ
-1	$CuFeS_2 + 3O_2(g) = CuFeO_2 + 2SO_2(g)$	-720.883	-932.68 + 0.189T
-2	$CuFeS_2 + 4O_2(g) = CuSO_4 + FeSO_4$	-746.15	-1507.98 + 0.710T
-3	$CuFeS_2 + 13/4O_2(g) = CuO + 1/2Fe_2O_3 + 2SO_2(g)$	-735.053	-980.77 + 0.229T
-4	$CuFeS_2 + 19/6O_2(g) = CuO + 1/3Fe_3O_4 + 2SO_2(g)$	-722.947	-938.65 + 0.201T
-5	$FeS_2 + 11/4O_2(g) = 1/2Fe_2O_3 + 2SO_2(g)$	-752.358	-831.76 + 0.074T
-6	$FeS_2 + 8/3O_2(g) = 1/3Fe_3O_4 + 2SO_2(g)$	-737.133	-790.79 + 0.050T
-7	$2FeS_2 + 7O_2(g) = Fe_2(SO_4)_3 + SO_2(g)$	-1489.25	-2530.06 + 0.970T
-8	$FeS_2 + 3O_2(g) = FeSO_4 + SO_2(g)$	-739.066	-1050.236 + 0.291T
-9	$PbS + 3/2O_2(g) = PbO + SO_2(g)$	-328.660	-414.50 + 0.080T
-10	$PbS + 2O_2(g) = PbO_2 + SO_2(g)$	-291.299	-479.10 + 0.175T
-11	$PbS + 2O_2(g) = PbSO_4$	-450.939	-812.54 + 0.337T
-12	$CuFeS_2 + 4O_2(g) + 2CaO = CuFeO_2 + 2CaSO_4$	-1.055.117	-1828.75 + 0.721T
-13	$CuFeS_2 + 17/4O_2(g) + 2CaO = CuO + 1/2Fe_2O_3 + 2CaSO_4$	-1.160.287	-1976.84 + 0.761T
-14	$FeS_2 + CaO + 13/4O_2(g) = 1/2Fe_2O_3 + CaSO_4 + SO_2(g)$	-961.799	-1329.89 + 0.343T
-15	$FeS_2 + 2CaO + 11/3O_2(g) = 1/3Fe_3O_4 + 2CaSO_4$	-1.162.734	-1787.22 + 0.582T
-16	$FeS_2 + 2CaO + 7/2O_2(g) = FeO + 2CaSO_4$	-1.096.548	-1690.99 + 0.554T
-17	$PbS + CaO + 2O_2(g) = PbO + CaSO_4$	-541.272	-912.53 + 0.346T
-18	$PbS + CaO + 5/2O_2(g) = PbO_2 + CaSO_4$	-501.812	-980.37 + 0.446T
-19	$Fe_2O_3 + CaO = CaO{\cdot}Fe_2O_3$	-41.771	305.930 – 0.324T
-20	$Fe_2O_3 + CaO = CaFe_2O_4$	-367.815	-26.065 – 0.01T
-21	$PbO + 2CaO + 1/2O_2(g) = Ca_2PbO_4$	69.974	-217.63 + 0.268T
-22	$PbO_2 + 2CaO = Ca_2PbO_4$	-10.891	-132.14 + 0.113T

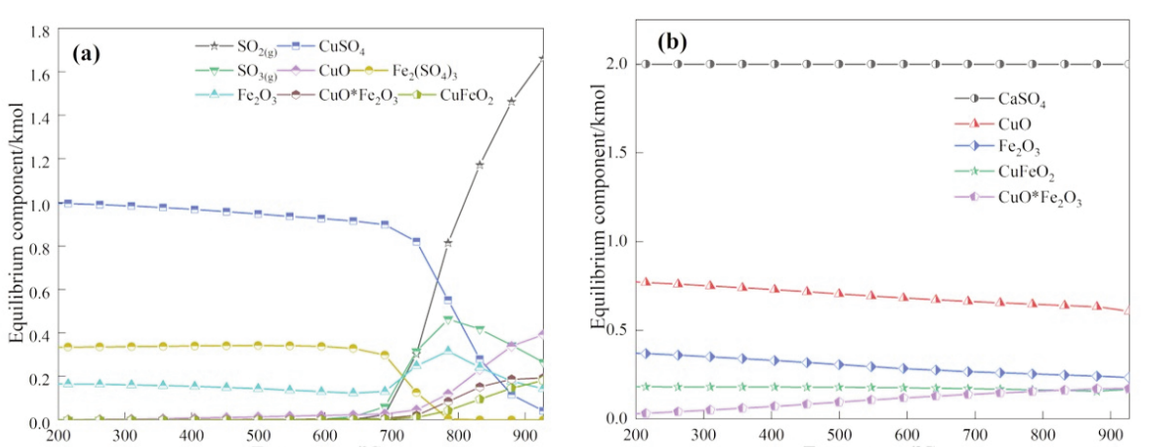

Figure 1. *Equilibrium composition diagram of chalcopyrite oxidation reaction: (a) without CaO, (b) with CaO*

the stable phases of the Pb-Ca-O-S system were $CaSO_4$ and PbO_2, and the stable phases of the Cu-Fe-Pb-O-S system were CuO, Fe_2O_3, and PbO_2 with a Po_2 value of about 104.33 Pa and a Pso_2 value of 10^{-8} to 10^{-4}, while the sulfur in the metal sulfide reacted with CaO and oxygen to form $CaSO_4$. That is, when using air to oxidize and roast LPCCO at 800 °C in the presence of CaO, the stable phases during the roasting process should be CuO, Fe_2O_3, PbO_2, and $CaSO_4$.

It should be noted that in the presence of CaO, PbO_2 was generated during the roasting process by reacting with CaO to generate Ca_2PbO_4, which were shown in equation (22) in Table 2. Due to the association of this chalcopyrite with lead, the formation of Ca_2PbO_4 may cover the surface of CuO, thereby impeding the acidic leaching of copper. During roasting, the presence of Ca_2PbO_4 phase in the product should be avoided.

3.2. The effects of roasting time

The pellets made from LPCCO mixed with CaO were roasted at 800 °C in air atmosphere for different periods, and the XRD patterns of the obtained calcine were shown in Figure 3. As can be seen in Figure 3, the main phase in the calcine obtained from roasting for 1 h without CaO was PbS, and the secondary phases were $PbSO_4$, Fe_2O_3, and $CuFeS_2$. However, in the presence of CaO, when calcined for 1 h, the main phases in the calcine were $CaSO_4$ and PbO_2, and the secondary phases were Fe_2O_3, CuO, and CaO, and none of the Ca_2PbO_4 was detected. In addition, when the roasting time was 2 hours, the phase of the calcined product was basically consistent with that of the calcined product for 1 hour. When the roasting time increased to 3 h, the main phases were $CaSO_4$ and Ca_2PbO_4, and the secondary phases were Fe_2O_3 and CuO, however, none of the PbO_2 was detected.

The XRD characterization results show that when calcined at 800 °C for 1 h, PbS and $CuFeS_2$ were not completely oxidized without adding of CaO, while FeS_2 could be completely oxidized to Fe_2O_3, which was consistent with the thermodynamic analysis mentioned above in this paper. When CaO with amount of 50.0 wt.% concentrate mass was added for mixing with

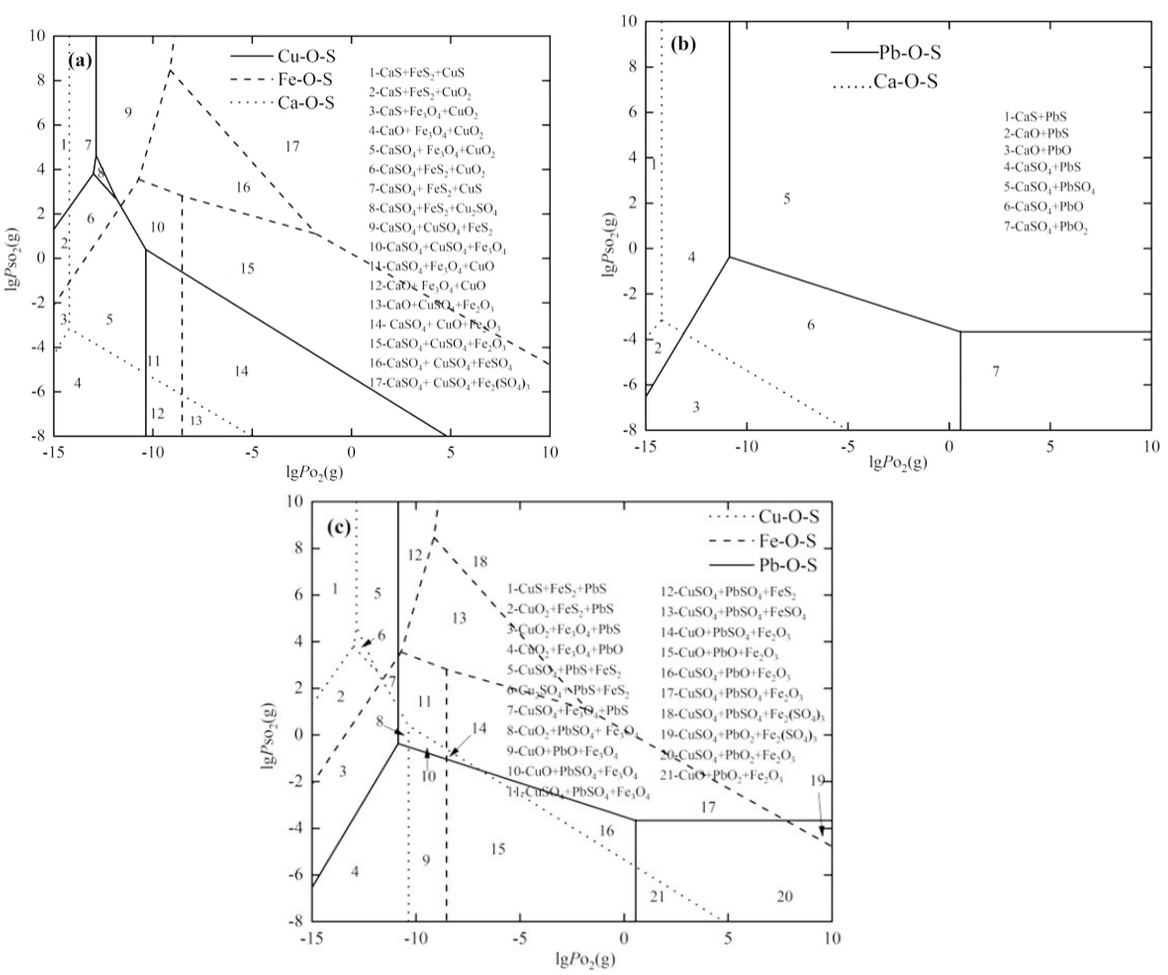

Figure 2. *Dominant zone diagram of different systems at 800 °C, (a): Cu-Fe-Ca-O-S system; (b): Pb-Ca-O-S system; (c): Cu-Fe-Pb-O-S system*

CC BY SA

LPCCO to roast for 1 h, it can promote the oxidation of $CuFeS_2$ and PbS, and convert the sulfur combined in the raw materials therein into $CaSO_4$, thereby playing a role in sulfur fixation. The phase of the product after roasting for 2 h did not change significantly compared to that of roasting for 1 h. When roasting for 3 hours, the PbO_2 generated during the roasting process reacted with excess of CaO to generate Ca_2PbO_4, which was not conducive to leaching copper. Therefore, it can be concluded that when the roasting time was 1 h, $CuFeS_2$ completely transformed into CuO that was easy to leach, and Ca_2PbO_4 was not detected, resulting with the optimal roasting time of 1 h.

3.3. The effects of pellet size

Different pellet sizes of LPCCO mixed with CaO were calcinated for 1 h at 800 ℃ in atmospheric environment for studying the effect of pellet sizes on the calcination, and the XRD patterns of the obtained calcines are shown in Figure 4. As can be seen in Figure 4, when the particle size of the pellet was 5.0 mm, the main phases in the calcination product were $CaSO_4$, PbO_2, Fe_2O_3, CuS·FeS, and CaO, and none PbS and FeS_2 were detected. This indicated that when the particle size of the pellet was 5.0 mm, FeS_2 and PbS were completely oxidized to Fe_2O_3 and PbO_2, while most of $CuFeS_2$ did not undergo oxidation under this particle size. When the particle size of the pellet was 10 mm, the main phases detected in the calcined product were $CaSO_4$, PbO_2, and Fe_2O_3, while the secondary phases were CuO and CaO. CuS·FeS was not detected, indicating that $CuFeS_2$ was completely oxidized to CuO and Fe_2O_3 at this time. When the particle size of the pellet was 20.0 mm, $CaSO_4$, PbO_2, Fe_2O_3, CuS·FeS, CaO, and $PbSO_4$ were detected in the calcined product, but no CuO was detected. However,

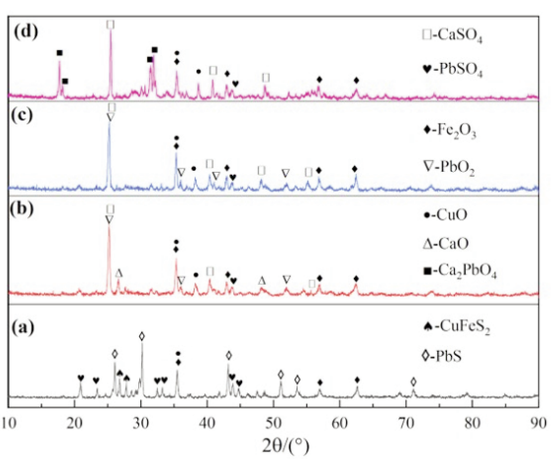

Figure 3. *XRD patterns of calcined products at different calcination times (pellet size=10 mm, Temperature=800 ℃); Roasting 1 h without Cao (a), roasting with CaO for 1 h (b), 2 h (c) and 3 h (d)*

the diffraction peak of CuS·FeS was significantly enhanced, and a new diffraction peak of $PbSO_4$ appeared, indicating that the incompletely oxidation of LPCCO under this particle size. The above test results indicated that too small or too large calcined pellet particle size was not conducive to the complete oxidation of $CuFeS_2$ [24]. Therefore, the optimal calcined pellet size was 10.0 mm.

3.4. Behavior of acid leaching

Acid leaching tests with stirring speed of 500 r/min for 1.5 h at 85 ℃ with the liquid-solid ratio of 5∶1 mL/g and mass concentration of sulfuric acid of 120 g/L were conducted with the calcines obtained under different conditions. The copper leaching rates

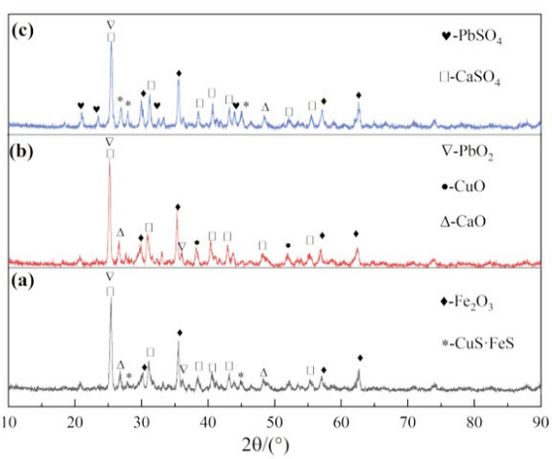

Figure 4. *XRD of calcined products with different pellet sizes (T=800 ℃, time 1 h) Pellet size 5.0 mm (a), 10.0 mm (b)and 20.0 mm (c)*

are shown in Figure 5. Figure 5 testifies that the optimal roasting time and pellet size were 1 h and 10 mm, respectively. Under these conditions, $CuFeS_2$ in the raw material could be more effectively converted into easily soluble CuO, and the copper leaching rate increased to 98.60 wt.%. With the prolongation of roasting time, the reason leading to the decrease in copper leaching rate may be that the product PbO_2 obtained from roasting reacted with excess CaO to generate Ca_2PbO_4, which was highly likely to cover the surface of CuO [25, 26].

In order to further study the effect of CaO on the acid leaching residue of calcine, XRD analysis was conducted

In order to further study the effect of CaO on the acid leaching residue of calcine, XRD analysis was conducted on the acid leaching residue of calcine, and the results are shown in Figure 6. Figure 6a indicates that the mineral phases in the acid leaching residue with calcine roasted without CaO were mainly $PbSO_4$ and $PbFe_6(OH)_{12}(SO_4)_4$. Figure 6b indicates that only

CC BY SA

$CaSO_4$ and $PbSO_4$ were detected in the acid leaching residue of calcine obtained in the presence of CaO.

3.5. Morphological characterization

The SEM and EDS characterization results of LPCCO, calcination products, and leaching residues are shown in Figure 7 and Table 3, respectively.

As can be seen from Figure 7 and Table 3, chalcopyrite, pyrite, and galena in the LPCCO were wrapped and embedded with each other, with a dense structure and complex composition. The structure of the calcined product was loose, and the main mineral phases were PbO_2, Fe_2O_3, CuO, and $CaSO_4$. EDS analysis showed that the mineral phase of the roasting products got after calcination was consistent with the thermodynamic analysis results mentioned above. The leaching residue obtained from acid leaching of calcined products under atmospheric pressure had a relatively dispersed particle distribution and became very fine, mainly consisting of $PbSO_4$ and $CaSO_4$. The vast majority of copper contained in calcine entered the leaching solution, which also indicated that adding of CaO could optimize the roasting process of LPCCO.

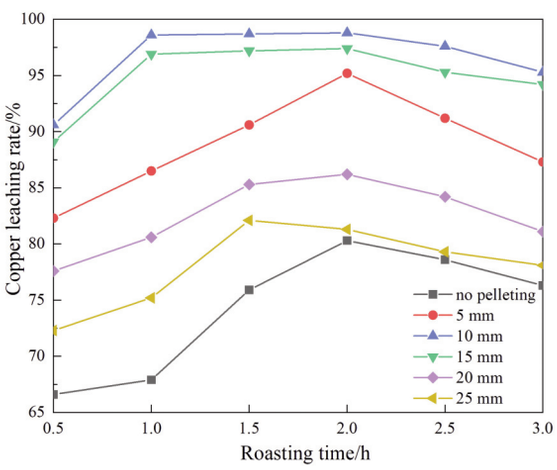

Figure 5. Effect of different roasting time and pellet size on copper leaching rate (800 °C)

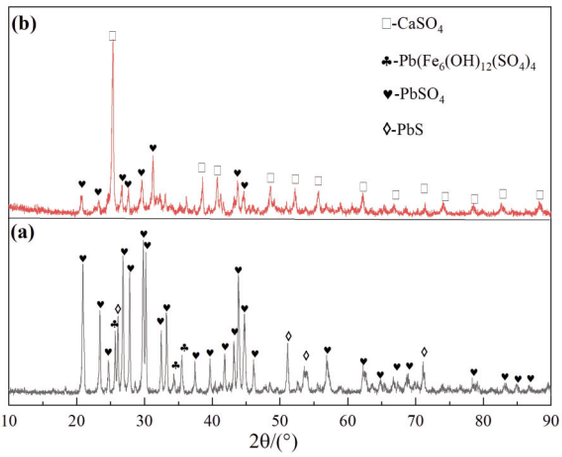

Figure 6. XRD patterns of leaching residue of calcine without adding CaO (a) and leaching residue calcine with CaO (b)

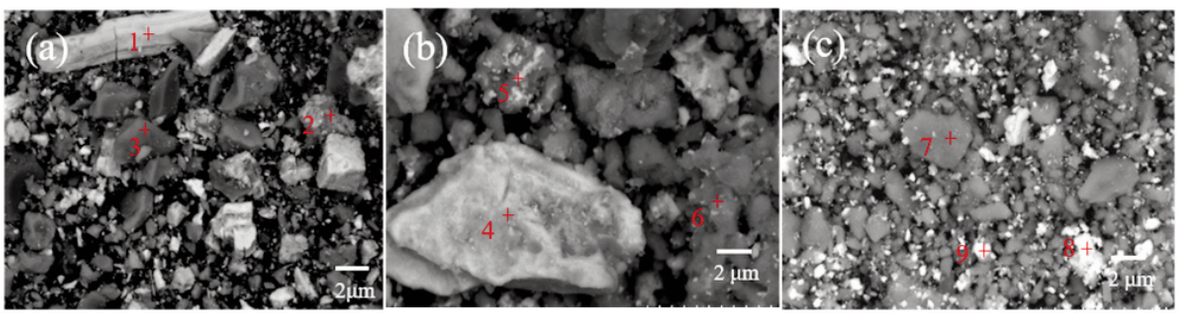

Figure 7. SEM images of raw ore(a), roasting product(b) and leaching residue(c)

Table 3. Results of EDS analysis of LPCCO, calcine roasting product and leaching residue

Sample	Spot	Element / wt.%					
		O	S	Ca	Fe	Cu	Pb
Raw ore	1	-	11.60	-	3.73	1.47	83.20
	2	-	13.35	-	5.55	2.01	50.09
	3	-	35.05	-	12.65	1.04	51.26
Roasting product	4	35.58	4.31	6.31	12.72	4.13	39.96
	5	46.68	13.74	19.18	5.92	2.01	12.46
	6	37.12	10.98	14.43	8.66	2.88	25.93
Residue	7	50.59	16.34	25.83	0.69	-	6.55
	8	34.05	5.60	10.24	1.72	-	48.39
	9	33.67	2.21	6.54	1.21	-	56.50

CC BY SA

4. Conclusions

(1) Thermodynamic analysis showed that selecting appropriate temperature and controlling sulfur and oxygen potentials could convert copper bearing minerals into CuO easily soluble in diluted acid, pyrite and galena into Fe_2O_3 and PbO_2, respectively, as well as S combined as metal sulfides in raw material was fixed in the obtained calcine with the form of $CaSO_4$.

(2) The optimal conditions for calcining LPCCO pelleted with CaO in a particle size of 10 mm was roasting time of 1 h at 800 ℃ and, $CuFeS_2$ in LPCCO was converted into easily soluble CuO and Fe_2O_3, and the sulfur in galena and pyrite was converted into $CaSO_4$ by reacting with calcium oxide in an oxidizing atmosphere. Too long roasting time led to the production of Ca_2PbO_4 which would hinder copper leaching.

(3) Using H_2SO_4-H_2O system to leach the calcine obtained under the optimal roasting conditions, the copper leaching rate could reach 98.60 wt.%.

Acknowledgments

The authors express the sincere appreciation to the financial support of the National Natural Science Foundation of China (Project No. 21978122).

Author contributions

H.-F. Ma: Investigation, Methodology, Software, Fitting, Formal analysis, Validation, Data curation, Writing–original draft. Y.-L. Liao: Resources, Supervision, Formulation of research ideas, Project administration, Paper modification and editing. M. Wu: Writing–review & editing. X.-B. Jia: Writing–review & editing. S.-Y. Yang: Writing – review & editing.

Declaration of interest statement

This article has not been published elsewhere in whole or in part. All authors have read and approved the content, and agree to submit for consideration for publication in the journal. There are no any ethical/legal conflicts involved in the article.

References

[1] H. B. Zhao, Y. S. Zhang, X. Zhang, L. Qian, M. L. Sun, Y. Yang, Y. S. Zhang, J. Wang, H. J. Kim, G. Z. Qiu, The dissolution and passivation mechanism of chalcopyrite in bioleaching: An overview, Minerals Engineering, 136 (2019) 140-154. https://doi.org/10.1016/j.mineng.2019.03.014

[2] Y. Wu, Y. L. Liao, G. X. Ji, Q. F. Liu, Study on thermal decomposition and its non-isothermal kinetics of chalcopyrite, Journal of Kunming University of Science and Technology (Natural Science Edition), 47(5) (2022) 10-21. https://doi.org/10.16112/j.cnki.53-1223/n.2022.05.202

[3] A. A. Baba, K. I. Ayinla, F. A. Adekola, M. K. Ghosh, O. S. Ayanda, R. B. Bale, A. R. Sheik, S. R. Pradhan, A review on novel techniques for chalcopyrite ore processing, International Journal of Mining Engineering and Mineral Processing, 1(1) (2012) 1-16. https://doi.org/10.5923/j.mining.20120101.01

[4] C. Li, Study on pressure leaching of chalcopyrite. (eds) Shenyang: Northeastern University, (2015) 1-93.

[5] S. K. Singh, A. W. Savoy, Ionic liquids synthesis and applications: an overview, Journal of Molecular Liquids, 297 (2019) 112038. https://doi.org/10.1016/j.molliq.2019.112038

[6] Z. Y. Tian, H. D. Li, Q. Wei, F. Jiao, W. Q. Qin, C. R. Yang, Effects of Cu2+, Fe2+, and Fe3+ on bioleaching of chalcopyrite by moderate thermophilic mixed bacteria, The Chinses Journal of Nonferrous Metals, 31(1) (2021) 171-180. https://doi.org/10.11817/j.ysxb.1004.0609.2021-37733

[7] X. M. Hua, Y. F. Zheng, Q. Xu, X. G. Lu, H. W. Cheng, X. L. Zhou, Q. S. Song, Z. Q. Ning, Interfacial reactions of chalcopyrite in ammonia-ammonium chloride solution, Transactions of Nonferrous Metals Society of China, 28(3) (2018) 556-556. https://doi.org/10.1016/S1003-6326(18)64688-6

[8] Q. Yin, D. J. Vaughan, E. R. Katharine, G. H. Kelsall, N. Brandon, Surface oxidation of chalcopyrite (CuFeS2) in alkaline solutions, Journal of the Electrochemical Society, 147(8) (2000) 2945-2951. https://doi.org/ 10.1149/1.1393629

[9] M. Ranjbar, M. H. Fazaelipoor, R. H. Mohammad, M. Schaffie, Z. Manafi, Modeling study of the bio-dissolution of coper concentrate in a continuous bioreactors system, Minerals Engineering, 153 (2020) 106384. https://doi.org/10.1016/j.mineng.2020.106384

[10] H. Zhang, D. Z. Wei, W. G. Liu, D. X. Hou, R. Y. Zhang, Effect of polyvinyl pyrrolidone on chalcopyrite bioleaching with acidithiobacillus ferrooxidans, Hydrometallurgy, 205 (2021) 105753. https://doi.org/10.1016/j.hydromet.2021.105753

[11] J. L. Xia, J. J. Song, H. C. Liu, Z. Y. Nie, L. Shen, P. Yuan, C. Y. Ma, L. Zheng, Y. D. Zhao, Study on catalytic mechanism of silver ions in bioleaching of chalcopyrite by SR-XRD and XANES, Hydrometallurgy, 180 (2018) 26-35. https://doi.org/10.1016/j.hydromet.2018.07.008

[12] H. B. Zhao, Y. S. Zhang, M. L. Sun, P. F. Ou, Y. J. Zhang, R. Liao, G. Z. Qiu, Catalytic mechanism of silver in the oxidative dissolution process of chalcopyrite: Experiment and DFT calculation, Hydrometallurgy, 187 (2019) 18-29. https://doi.org/10.1016/j.hydromet.2019.05.002

[13] H. Nourmohamadi, M. D. Esrafili, V. Aghazadeh, DFT study of ferric ion interaction with passive layer on chalcopyrite surface: Elemental sulfur, defective sulfur and replacement of M^{2+}(M=Cu and Fe) ions, Computational Condensed Matter, 26 (2021) e00536. https://doi.org/10.1016/j.cocom.2021.e00536

[14] S. F. Wu, C. R. Yang, W. Q. Qin, F. Jiao, J. Wang, Y. S. Zhang, Sulfur composition on surface of chalcopyrite during its bioleaching at 50 ℃, Transactions of Nonferrous Metals Society of China, 25(12) (2015) 4110-4118. https://doi.org/101016/S1003—

6326f15)64062-6

[15] M. K. Coruh, M. Çopur, The connection calcination and sulphation with the thermal behavior of chalcopyrite ore concentrate, Press Academia Procedia, 5(1) (2017) 214-223. https://doi.org/10.17261/Pressacademia.2017.592

[16] Z. L. Ye, Z. Shi, Y. F. Shi, B. Q. Zhang, H. K. Dai, Research on oxygen pressure acid leaching of sulfidized chalcopyrite, Journal of Kunming University of Science and Technology (Natural Science Edition), 39(2) (2014) 1-6. https://doi.org/10.3969 /j.issn.1007-855x.2014.02.001

[17] J. Luo, G. H. Li, Z. W. Peng, M. J. Rao, Y. B. Zhang, T. Jiang, Phase evolution and Ni-Fe granular growth of saprolitic laterite ore–CaO mixtures during reductive roasting, JOM, 68(12) (2021) 3015-3021. https://doi.org/10.1007/s11837-016-2118-4

[18] R. Padilla, M. Rodriguez, M. C. Ruiz, Sulfidation of chalcopyrite with elemental sulfur, Metallurgical and Materials Transactions B: Process Metallurgy and Materials Processing Science, 34(1) (2003) 15-23. https://doi.org/10.1007/s11663-003-0050-9

[19] Y. Di, Y. Zhang, Y. S. Wu, Phase equilibrium calculation of CO2-hydrocarbons-water system based on Gibbs free energy minimization, Acta Petrolei Sinica, 36(5) (2015) 593-599. https://doi.org/10.7623/syxb201505008

[20] B. B. Xie, B. B. Hu, L. F. Jiang, G. Li, Z. L. Du, The phase transformation of $CuInS_2$ from chalcopyrite to wurtzite, Nanoscale Research Letters, 10(01) (2015) 56. https://doi.org/10.1186/s11671-015-0800-z

[21] Y. Zhang, J. Wang, B. Liu, J. Huang, J. Ye, Y. Li, Z. Su, J. Wang, Extraction and separation of Mn and Pb from electrolytic manganese anodic slime (EMAS) via SO_2 roasting followed by acid leaching process, JOM, 72(2) (2020) 925-932. https://doi.org/10.1007/s11837-019-03650-1

[22] S. Ahmad, W. R. Sajal, F. Gulshan, M. Hasan, M. A. Rhamdhani, Thermodynamic analysis of caustic–roasting of electric arc furnace dust, Heliyon, 8 (2022) e11031. https://doi.org/10.1016/j.heliyon.2022.e11031

[23] Z. Ouyang, Y. F. Chen, S. Y. Tian, L. Xiao, C. B. Tang, Y. J. Hu, Z. M. Xia, Y. M. Chen, L. G. Ye, Thermodynamic and kinetics analysis of the sulfur-fixed roasting of antimony sulfide using ZnO as sulfur-fixing agent, Journal of Mining and Metallurgy Section B-Metallurgy, 54 (3) B (2018) 411–418. https://doi.org/10.2298/JMMB180510031o

[24] D. Q. Zhu, X. Hu, J. Pan, C. C. Yang, M. J. Xu, Z. Y. Wang, Optimization of feed blends to enhance the performance of pellets made from Western Australian ultrafine magnetite concentrate, Journal of University of Science and Technology Beijing, 39 (5) (2017) 683-392. https://doi.org/10.13374/j.issn2095-9389.2017.05.006

[25] X. J. Li, Research on spinels growth law and calcification roasting mechanism of vanadium slag. (eds) Chongqing: Chongqing University (2011) 1-72.

[26] S. C. Wang, X. F. Shi, Q. R. Zhang, K. Zhao, Roasting and induration mechanism in magnesia pellet, Iron Steel Vanadium Titanium, 39(5) (2018) 79-85. https://doi.org/10.7513/j.issn.1004-7638.2018.05.014

MEHANIZAM FAZNE TRANSFORMACIJE KOD OKSIDACIONOG PRŽENJA SIROMAŠNE POLIMETALIČNE HALKOPIRITNE RUDE U PRISUSTVU CaO

H.-F. Ma, Y.-L. Liao *, M. Wu, X.-B. Jia, S.-Y. Yang

Fakultet za metalurgiju i energetsko inženjerstvo, Univerzitet za nauku i tehnologiju u Kunmingu, Kunming, Kina

Apstrakt

Siromašna polimetalična halkopiritna ruda ima visok sadržaj olova i gvožđa, kao i nisku tačku omekšavanja, što je čini teškom za obradu tradicionalnim pirometalurškim i hidrometalurškim procesima. Da bi se proučila odgovarajuća metodologija za efikasno iskorišćenje, u ovom radu je izvršeno peletiranje s dodatkom CaO za proces oksidacionog prženja. Kontrolom Po_2 i Pso_2 u gasnoj fazi, sulfid metala u rudi se transformiše u lako rastvoriv oksid metala. Izvršena je termalna analiza procesa prženja, a proučeno je i kiselinsko luženje dobijenog kalcinata na atmosferskom pritisku. Rezultati pokazuju da se peletiranjem sa CaO i zatim prženjem na 800 °C tokom 1 sata halkopirit transformiše u CuO, koji se lako rastvara, galenit i pirit transformišu se u PbO_2 i Fe_2O_3, dok sumpor reaguje sa CaO i pretvara se u $CaSO_4$, što fiksira sumpor u kalcinatu. Stopa luženja bakra u kalcinatu može dostići 98,60% pod atmosferskim pritiskom u H_2SO_4-H_2O sistemu. CaO može povećati tačku omekšavanja sirovina, poboljšati efekat prženja, podstaknuti faznu transformaciju halkopirita u procesu oksidacije i prevesti sumpor u $CaSO_4$ kako bi se efikasno izbeglo zagađenje okoline SO_2 gasom.

Ključne reči: *Halkopirit niskog kvaliteta; Kalcinaciono prženje; Oksidaciono prženje; Fazna transformacija; Kiselo luženje*